Early-stage aggregation in three-dimensional charged granular gas

Chamkor Singh[1,2] and Marco G. Mazza[1]

[1]*Max Planck Institute for Dynamics and Self-Organization (MPIDS), Am Faßberg 17, 37077, Göttingen, Germany*
[2]*Georg-August-Universität Göttingen, Friedrich-Hund-Platz 1, 37077 Göttingen, Germany*

Neutral grains made of the same dielectric material can attain considerable charges due to collisions and generate long-range interactions. We perform molecular dynamic simulations in three dimensions for a dilute, freely cooling granular gas of viscoelastic particles that exchange charges during collisions. As compared to the case of clustering of viscoelastic particles solely due to dissipation, we find that the electrostatic interactions due to collisional charging alter the characteristic size, morphology, and growth rate of the clusters. The average cluster size grows with time as a power law, whose exponent is relatively larger in the charged gas than the neutral case. The growth of the average cluster size is found to be independent of the ratio of characteristic Coulomb to kinetic energy, or equivalently, of the typical Bjerrum length. However, this ratio alters the crossover time of the growth. Both simulations and mean-field calculations based on Smoluchowski's equation suggest that a suppression of particle diffusion due to the electrostatic interactions helps in the aggregation process.

I. INTRODUCTION

Since classical antiquity lightnings have been associated with the ashes produced during volcanic activity [1,2]. It has been long speculated that collisional charging may play a significant role in particle's aggregation [3,4] in natural processes such as the formation of planetesimals during the early stages of the birth of a planet [4,5], charging in dust devils [6], lightenings in thunderclouds [7], and electric sparks in dunes [8]. At such length scales (10^2–10^4 m), a number of processes are observed such as charge separation, buildup of significant potential differences and electric discharge [9]. A specific example is the *electrostatic re-accretion* in the protoplanetary disks where the charged fragmented ejecta from a larger body are re-attracted toward the parent body due to its electrostatic field [10]. On a more mundane scale, this phenomenon also affects the processes at length scales which are technologically relevant, e.g., in vibrated granular beds [11], in transportation of coal [12], and in electrostatic powder spraying [13]. The origin of the above intriguing processes inside a granular gas is due to the charging of particles during collisions. This phenomenon, however, is rather stochastic as indicated by experimental measurements [5,14,15]. On the other hand, the consequences of this local exchange on a collection of particles have been experimentally observed to be quite complex as it shows highly fluctuating characteristics [16]. Very recently, these fluctuations also shown numerically in dense granular systems [17]. The collective consequences on particle aggregation and their growth due to this very local charge exchange in dilute granular system, however, are not yet well understood. Relevant exceptions are the theoretical findings in Refs. [18,19] for a *monopolarly* charged granular gas neglecting collisional charging, and the Smoluchowski's aggregation analysis in Ref. [20] for the *monopolarly* charged suspensions undergoing Brownian motion.

A granular gas is an adequate theoretical setup to study such particle aggregation processes in the dilute limit. The clusters in a *neutral* granular gas typically exhibit a power law growth during its time evolution [21,22]. It is, however, unclear if bipolar *collisional* charging of grains, which is ubiquitous in technological settings [11–13,23,24], and in natural flows [10,25–27], enhances or suppresses the cluster growth.

The dissipation in neutral granular gases leads to the formation of clusters. The growth of these clusters in two and three dimensions has been investigated in the past [28–31]. In three-dimensions, it is found that the cluster growth can be described by a power-law behavior with similar exponents as in percolation theory [28]. The same is shown for the growing clusters in two dimensions [29]. Furthermore, the coagulation equations for inelastic dust particles in a surrounding molecular gas, which is more relevant to natural settings, has also been studied from a mean-field point of view [31]. The growth of the clusters in granular gases has also been investigated for different nature of the interactions between the particles for example under short-range attractive potentials [32] and square well potential [33].

In this study we show that the time dependent average cluster size $S(t)$ in a charged granular gas obeys the power law

$$S(t) \sim t^z. \qquad (1)$$

We elucidate that (*i*) the early stage aggregation after the homogeneous cooling state (HCS) of the granular gas is relatively enhanced due to the *collisional* charging with z changing from $\approx 6/5$ for the *uncharged* gas to $\approx 3/2$ for the *charged* gas, (*ii*) the growth exponent z is found to be independent of the ratio of the characteristic Coulomb to kinetic energy $\mathcal{K}$ or equivalently the ratio $\mathcal{K} = \ell_B/d$ of the Bjerrum length $\ell_B = k_e q_{ref}^2/T_0$ to the particle diameter d, where q_{ref} is the typical charge on the particles, T_0 the kinetic energy scale or the granular temperature, and $k_e = 1/(4\pi\varepsilon_0)$ is the Coulomb constant with vacuum permittivity $\varepsilon_0 = 8.85418782 \times 10^{-12}$ F m^{-1}. A change in ℓ_B, however, influences the characteristic time

of emergence of clustering. (*iii*) We find that contrary to the case of neutral viscoelastic particles, the velocity distribution of the charged viscoelastic particles does not show a relaxation back towards the Maxwellian within the characteristic time of emergence of the inhomogeneous cooling state (ICS).

II. MODEL

To model the charged granular gas, we employ Hertzian elastic forces, nonlinearly dissipative viscoelastic model [34–36] and the classical Coulomb forces in the framework of granular molecular dynamics (MD) in three dimensions. We numerically integrate the following form of Newton's equation of motion for the position $\boldsymbol{r}_i^*$ of a particle,

$$\ddot{\boldsymbol{r}}_i^*(t^*) = \sum_j \left[\Theta(\xi_{ij}^*) \left(\mathcal{E} \xi_{ij}^{*\frac{3}{2}} - \mathcal{D} \xi_{ij}^{*\frac{1}{2}} \dot{\xi}_{ij}^* \right) \boldsymbol{n}_{ji} \right]$$
$$+ \mathcal{K} \sum_{k, k \neq i} \frac{q_i^* q_k^*}{r_{ki}^{*2}} \boldsymbol{n}_{ki} , \qquad (2)$$

where $\xi_{ij} = d - |\boldsymbol{r}_i - \boldsymbol{r}_j|$ is the overlap distance due to viscoelastic deformation of a particle i upon collision with particle j, $\Theta(\xi_{ij})$ is the Heaviside step function ($\Theta(\xi_{ij}) = 1$ if $\xi_{ij} \geqslant 0$, and 0, otherwise), $\boldsymbol{n}_{ji} = \boldsymbol{r}_{ji}/r_{ji}$ (with $\boldsymbol{r}_{ji} = \boldsymbol{r}_i - \boldsymbol{r}_j$, $r_{ji} = |\boldsymbol{r}_{ji}|$) is the unit vector pointing from the center of particle j toward the center of particle i, and q^* is the charge on the particles at time t^*. The symbol $*$ indicates that we measure length, mass, time and charge in units of particle diameter d, mass m, reference time $\sqrt{md^2/T_0}$, and a reference charge $q_{\rm ref}$ discussed below, respectively. The nondimensional parameter $\mathcal{E} = \alpha d^{5/2}/T_0$ represents the ratio of characteristic elastic to kinetic energy, and $\mathcal{D} = \alpha A d^{3/2}/\sqrt{mT_0}$ the ratio of characteristic viscous to kinetic energy. The coefficient $\alpha = \frac{2Y}{3(1-\nu^2)}\sqrt{R_{\rm eff}}$ collects material and geometric properties namely Young's modulus Y, Poisson's ratio ν and the effective radius $R_{\rm eff} \equiv R_i R_j/(R_i + R_j)$ of the colliding pair [36]. The constant A is a material parameter that depends on the viscous properties of the particles [36]. The dissipative term in Eq. (2) takes into account a coefficient of restitution ϵ, which depends upon the impact velocity. ϵ is the fractional reduction in the normal component of the relative velocities of colliding particles, and reads $\epsilon = \dot{\xi}^{*\prime}_{ij}/\dot{\xi}^*_{ij}$ where $\dot{\xi}^*_{ij}$ and $\dot{\xi}^{*\prime}_{ij}$ are the relative normal velocities of the particles just before and after the contact. The granular temperature $T_{\rm g}(t) = \frac{1}{3}m\langle [\boldsymbol{v}_i(t) - \langle \boldsymbol{v}(t)\rangle]^2\rangle$ at $t = 0$ is chosen as the energy scale T_0, i.e., $T_0 \equiv T_{\rm g}(0)$, where $\boldsymbol{v}$ are the particle velocities. Because the elastic and dissipative parts in Eq. (2) are contact forces, the first sum extends only to particles j in contact with particle i, while the second some extends over all the particles k with $k \neq i$.

We simulate $N \sim 10^4$–10^5 identical, viscoelastic particles in a three-dimensional domain of volume $V = L^3$. The filling fraction of the system $\phi \equiv N\pi d^3/(6V) = 0.076$ and the ratio $\mathcal{E}/\mathcal{D} \approx 10$ are kept constant [37] while the effect of $\mathcal{K} = \ell_{\rm B}/d$ on the particle aggregation is studied, with $\mathcal{K} = 0$ corresponding to the neutral viscoelastic granular gas. In addition, the particles attain charge during the pairwise collisions according to a charge exchange rule, discussed below.

Collisional charging has far-reaching consequences. Large amounts of charges are generated in volcanic plumes [1];

estimated figures are of the order of 10^5 or 10^6 elementary charges per cubic centimeter [1], and this effect might have played a role for the origin of life by synthesizing amino acids [38]. Dust and sand storms also exhibit contact electrification and lightnings [39–41], and such phenomena might even exist on Mars [42]. Contact electrification can result in explosions if a flammable material is present [12,41,43]; pharmaceutical processes are often plagued by electrostatic charge buildup [23,44] leading to high maintenance costs. Understandably, a vast amount of attention has been put to explore what mechanisms stimulate the charge buildup, separation, transport, and its effect on the dynamics of granular flows [1,3,8,17,24,45]. Additionally, the collective behavior is are unclear in spite of great experimental [5,14,16,16] and theoretical [11,17–19,46] efforts. Moreover, the theory of contact electrification, i.e., charging of similar or dissimilar surfaces due to mutual contact is not yet rigorously established. Two basic, experimental facts still defy a consistent explanation: (*i*) insulators can transfer large amounts of charge, though they have no free charge carriers; (*ii*) upon contact and impact even the grains with identical material charge up [45]. However, there are certain observations which have been made repeatedly in the context of collisional charging. For instance, an extensive and systematic experimental study conducted by Poppe *et al.* [5] has revealed that the number of elementary charges transferred during a collision of silica particles on polished quartz and silicon wafer surfaces, on average, are proportional to a power of the relative kinetic energy during the collision, i.e., $Z_{i \leftrightarrow j} = (CE_{\rm kin})^\kappa$, where $E_{\rm kin}$ is the relative kinetic energy during the collision and C [J^{-1}] ($C^{-1} \sim 10^{-12} - 10^{-15}$J) and $\kappa = 0.83$ are constants [5]. Similar observations have also been made in Ref. [15] for single collisions of glass particles exhibiting dependence of charge transfer on impact energy. This, in one sense, is analogous with the impact velocity-dependent coefficient of restitution. However, the widespread nature of data in the collisional charging experiments also suggests that the collisional charge exchange is influenced by myriad factors. Indeed, among possible influential parameters are the surface material and its roughness, contact pressure, surface cleaning, humidity, the orientation of the crystalline lattice, the temperature of the surfaces, and the size of the colliding objects [5]. Taking this into account, we introduce a collisional impact energy dependent model for the charge exchange augmented by a stochasticity in its parameters

$$q_{i \leftrightarrow j} = \pm e Z_{i \leftrightarrow j} = \pm e \left[\Psi_1 C \tfrac{1}{2} m_{\rm eff} \dot{\xi}_{ij}^2 \right]^{\kappa + \Psi_2}, \qquad (3)$$

or in nondimensional terms

$$q_{i \leftrightarrow j}^* = \pm \mathcal{Q} \left[\Psi_1 m_{\rm eff}^* \dot{\xi}_{ij}^{*2} \right]^{\kappa + \Psi_2}, \qquad (4)$$

where $\mathcal{Q} = \frac{e(Cmv_{\rm ref}^2)^\kappa}{q_{\rm ref}} = \frac{e(CT_0)^\kappa}{q_{\rm ref}}$, $m_{\rm eff} = m_i m_j/(m_i + m_j)$ is the reduced mass of the colliding particles, $e = 1.6021765 \times 10^{-19}$ C is the absolute value of the electron charge, Z is the number of elementary charges exchanged, $mv_{\rm ref}^2 = T_0$ is the kinetic energy scale. In our calculations, we fix $q_{\rm ref}$ such that $\mathcal{Q} \sim eC$. The numbers Ψ_1 and Ψ_2 are equally distributed noise with $\langle \Psi_1 \rangle = 1.63$, $\langle \Psi_2 \rangle = 0$, in the intervals $\Psi_1 \in [0.1, 3.1623]$ and $\Psi_2 \in [\kappa - 0.05\kappa, \kappa + 0.05\kappa]$. The mean and the interval of the noise Ψ_1 are chosen such that the charge exchange $q_{i \leftrightarrow j}$ fits the experimental power law $eZ_{i \leftrightarrow j} = e(CE_{\rm kin})^\kappa$ found in Ref. [5].

The multiplicative noise Ψ_1 indicates that the charge exchange in the system has a dependence on the current state of the kinetic energies of collisions while the stochasticity in the exponent does not depend on the kinetic conditions, which is reflected through an additive noise Ψ_2. In other words, in a freely cooling granular gas, where the impact kinetic energies keep decreasing over time, the stochastic coupling coefficient Ψ_1 assures an upper limit to the charge on an individual particle and avoids any unphysical divergence of the amount of charge on it. It should be noted that here we make the simplifying assumption, in lack of any established theory of tribocharging, that the charge exchange is independent of the preexisting charge on the particles before the collisions. This simplification is partially based on the experiments in Ref. [47], where it was observed that even precharged particles acquire additional charge upon collision, indicating a negligible influence of electrical conductance during the short collision time. Therefore, neglecting the possibility of discharging of the particles due to the combined effect of potential created by the preexisting charge and the electrical conductivity of the particle's material is a reasonable simplification. The addition of the stochastic variable Ψ_2 in the exponent is based on the fact that its value is reported to be fluctuating (0.83 in Ref. [5] while later 0.79 in Ref. [47]).

To minimize the finite size effects, we use the customary periodic boundary conditions. This choice effectively means that the system is replicated infinite times along each Cartesian axis. Because of the long-range nature of Coulomb's force, all periodic images of $k \neq i$ contribute to the electrostatic force on i. For a periodic domain, then, the Coulomb force $\boldsymbol{F}_i^{*(\mathrm{C})}$ on a particle i reads

$$\boldsymbol{F}_i^{*(\mathrm{C})} = k_e q_i^* \sum_{k=1}^{N} \sum_{\boldsymbol{b}}{}' \frac{q_k^*}{|\boldsymbol{r}_{ki}^* + \boldsymbol{b}L|^3}(\boldsymbol{r}_{ki}^* + \boldsymbol{b}L), \qquad (5)$$

where $\boldsymbol{b} = (b_x, b_y, b_z)$ is a vector of integers ($\in \mathbb{Z}$) representing the periodic replicas of the system in each Cartesian direction. The $'$ symbol indicates that $k \neq i$ if and only if $\boldsymbol{b} = \boldsymbol{0}$ to avoid Coulomb interaction of particles with themselves. The long-range Coulomb force sum in Eq. (5) for a setup with periodic boundary conditions is challenging and conditionally convergent as it depends on the order of summation. We employ the Ewald summation that converges rapidly, and has a computational complexity $\mathcal{O}(N^{3/2})$ [48]. The Ewald summation breaks the calculation into two sums, one in the real space and the other in Fourier/reciprocal space. We consider the minimum image convention for the real part of the sum while consider 16 Fourier replicas in each Cartesian direction. The algorithm is parallelized and highly optimized on graphics processing unit (GPU). In our simulations, the total computing time to reach simulation time $t^* \sim 10^3$ for a typical simulation with $N \sim 10^5$, including the long-range electrostatic forces, is of the order of weeks. Due to the existence of long-range interactions, the trajectories of the particles are essentially non-ballistic. This prevents the usage of event driven algorithms. We employ the velocity-Verlet algorithm to integrate Newton's equations. The simulations are initialized by randomly placing the particles in a 3D domain with initial velocities distributed according to a Gaussian with zero mean and $\sqrt{T_0}$ standard deviation. Any remaining, initial net velocity of the system $\sum_{i=1}^{N} v_i$ is removed to ensure that no net macroscopic flux is
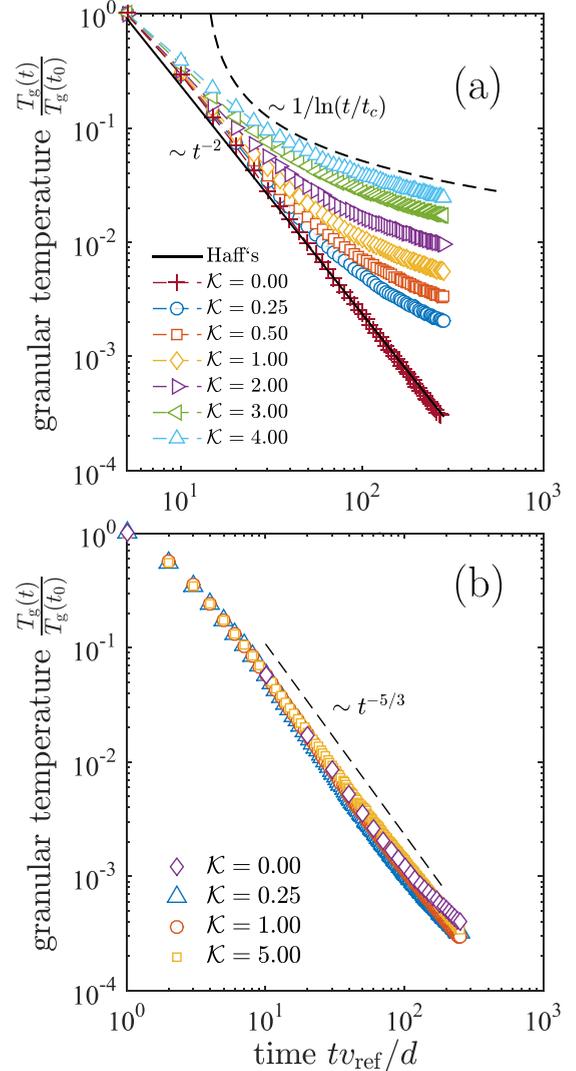
FIG. 1. (a) The evolution of the granular temperature T_{g} for a purely repulsive dilute granular gas with *monopolarly* charged particles and constant coefficient of restitution $\epsilon = 0.85$. We study the dependence on the ratio of characteristic Coulomb to kinetic energy $\mathcal{K}$. The $\mathcal{K} = 0$ curve corresponds to a neutral granular gas. At very short times, the granular gas follows Haff's law [$T_{\mathrm{g}}(t) \sim t^{-2}$] in the homogeneous cooling state. The repulsive electrostatic interactions among the particles reduce the collision frequency and thus result in a slower decay of T_{g} as time progresses [$T_{\mathrm{g}}(t) \sim 1/\ln(t/t_c)$, also shown analytically in Ref. [18], where t_c is the characteristic time separating power law from inverse logarithmic decay]. As $\mathcal{K}$ increases, the deviation from Haff's law is more pronounced and occurs earlier in time. The solid line represents the theoretical prediction of Haff's law for a neutral granular gas with $\epsilon = \mathrm{const.}$, and the dashed line is a theoretical prediction for monopolarly charged granular gases. (b) Same as (a) but for early stage of evolution of the viscoelastic ($\epsilon \neq \mathrm{const.}$) granular gas with charge exchange. The dashed line represents the theoretical prediction of Haff's law for a neutral viscoelastic granular gas.

present in our system. Initially, all particles have zero charge. We also ensure that the system is at all times globally neutral, i.e., $\sum_{i=1}^{N} q_i = 0$, by enforcing conservation of charge during each collision event. We let the system equilibrate for some
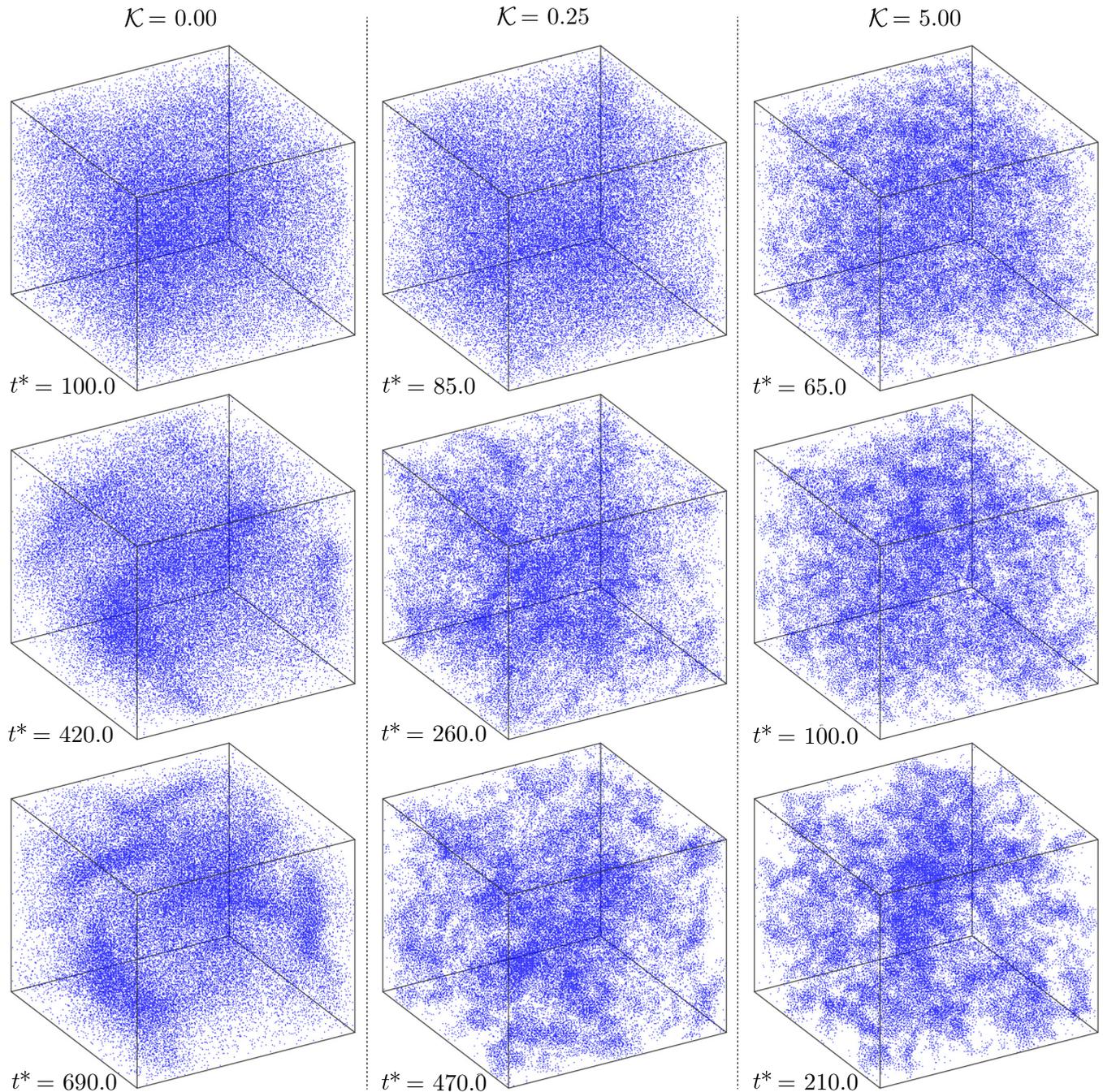
FIG. 2. Snapshots of the granular gas showing the time evolution of the *neutral* system of viscoelastic particles (left column) and *charged* viscoelastic particles (center and right columns). Here time $t^* = t v_{\mathrm{ref}}/d$, particle number $N = 50\,016$ and the particle filling fraction in the system $\phi = 0.076$. As the ratio of characteristic Coulomb to kinetic energy $\mathcal{K}$ increases, the characteristic time for the emergence of clustering decreases, however, their growth rate is unchanged (see also Fig. 5). The clusters exhibit a relatively compact morphology in the charged system.

time (marked as t_0) only under the influence of elastic forces. The dissipation and collisional charging is then switched on. For the sake of simplicity, we remove the $*$ symbols in the following.

III. RESULTS AND DISCUSSION

The dynamics of granular gases in the absence of electrostatics are reasonably well understood [49–53] and exhibit numerous intriguing features, such as universal Gaussian velocity distributions in the long time limit [49], multiscaling and self-similarity in collisions [54,55], nonequilibrium steady states and asymmetric velocity distributions under energy inputs [51], anomalous diffusion [56,57], ballistic aggregation of clusters as a whole [21], and dissimilarity between ensemble-averages and long-time averages of observables (nonergodicity) [58]. In addition, it is now known from Refs. [18,19,46] that if a granular gas is composed of
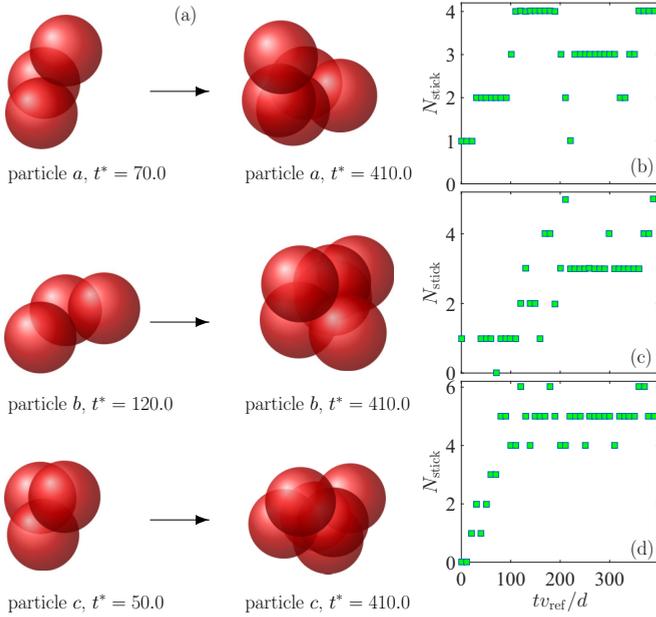
FIG. 3. Sticking of particles during clustering in the charged system. We observe a mechanism similar to *collide-and-capture* events observed in experiments on a falling granular stream in Ref. [14]. Particles stick together in clusters and exhibit pronounced persistence in each cluster over a considerable duration of time. This mechanism is not observed in the neutral system, where instead particles collide and separate. (a) Specific particles and their first neighbors are shown at different times. (b)–(d) The evolution of the number of contacts, N_{stick}, with time for the same particles shown in panel (a). The occasional *fragmentation* results in the fluctuation of N_{stick} with time.

equally charged particles (that is, the charge on each particle is equal in sign and magnitude), the number of collisions per unit time decreases due to the Coulomb repulsions. This, in comparison to a neutral granular gas, results in a slower decay rate of the kinetic energy per particle or the granular temperature T_g as the time progresses. This feature is recovered in our simulations as depicted in Fig. 1(a), which shows the decay of T_g with time for constant coefficient of restitution. At short times, the granular temperature follows Haff's law [$T_g(t) \sim t^{-2}$] [59,60], however at later times, it deviates from it and approaches a slower, inverse logarithmic scaling as was shown analytically in Ref. [18]. Moreover, the HCS becomes unstable due to dissipative cooling of the granular gas, and clustering emerges. Here we show that the additional perturbations due to collisional charging alters the geometrical morphology of clusters and their growth in time.

Figure 2 shows the time snapshots of the system for both neutral ($\mathcal{K} = 0.0$) and charged viscoelastic granular gas ($\mathcal{K} = 0.25$ and 5.0). The clusters are relatively elongated for neutral viscoelastic systems, while they are relatively compact in the collisionally charged system. The clustering for nonzero $\mathcal{K}$ initiates through mutual sticking of charged particles and results in the formation of very localized agglomerates of particles (Fig. 3). This agglomeration process is identified by following the trajectories of particles and, via nearest-neighbor search, identifying the particles which are in contact with

the followed particle. A contact is defined if $|\boldsymbol{r}_{ij}| \leqslant d$. As the time progresses, we see that there is a definite trend of particles to stick together [see Fig. 3(a)], and the persistence of individual particles in these localized aggregates is rather long lived [Figs. 3(b)–3(d)]. The long persistence of particle contacts is not present in the ICS of the neutral granular gas where particles aggregate due to a mechanism described as a hydrodynamic instability [50]. In fact, a *collide-and-capture* mechanism has been observed experimentally in Ref. [14], for collisional charging in a falling dilute granular stream. In the experiments [14], the particles collide, bounce multiple times, and then tend to stick together giving rise to local aggregates. One particular observation made in Ref. [14] is that when a single particle hits a cluster, it can either get *trapped* in the electrostatic field or can cause other particles to leave the cluster leading to fragmentation. In our simulations, the fragmentation is observed occasionally as suggested by fluctuating neighbor contacts N_{stick} in [Figs. 3(b)–3(d)] over time.

Figure 4(a) shows the time evolution of the mean absolute charge, $\bar{q} = \frac{1}{N} \sum_{i=1}^{N} |q_i|$, in the system. According to our ansatz, the rate and extent of collisional charging strongly depend on the number of collisions occurring per unit time, as well as on the relative velocities between the colliding particles. Due to dissipation, on the other hand, the kinetic energies of the particles keep decreasing and thus effectively contributing to the reduction of charge exchange between the particles. Once the kinetic energy per particle becomes sufficiently low, the mean charge in the system begins to saturate. The initial evolution of the mean charge can be estimated by the product of the initial collision frequency ω and the charge exchange during single collision $q_{i \leftrightarrow j}$. Since initially all particles are neutral, the collision frequency must coincide with its neutral counterpart $\omega(t = 0) = n\pi\sigma^2 \langle \dot{\xi}_{12} \rangle$ [18], where $\langle \dot{\xi}_{12} \rangle$ is the mean relative velocity between colliding particles, n is the number density, and $\sigma = d$ is the impact parameter. Then the initial rate of collisional charge exchange is

$$\omega \langle q_{i \leftrightarrow j} \rangle = n\pi\sigma^2 \langle \dot{\xi}_{12} \rangle \left[C m_{\text{eff}} \langle \dot{\xi}_{12}^2 \rangle \right]^\kappa e, \qquad (6)$$

which is proportional to the rate of mean collisional charging $\dot{\bar{q}}$. Assuming initially a Gaussian velocity distribution, so that $\langle \dot{\xi}_{12} \rangle \propto T_g^{1/2}$, and considering the fact that for viscoelastic particles $T_g \propto t^{-5/3}$, the evolution of $\bar{q}$ obeys

$$\dot{\bar{q}} \propto T_g^{1/2} T_g^\kappa \propto t^{-5/6} t^{-5/(3\kappa)}. \qquad (7)$$

As experiments show that $\kappa \approx 0.8$ [5], the rate of mean charge buildup with time is then

$$\dot{\bar{q}} \propto t^{-13/6}. \qquad (8)$$

A fit of the simulation results to Eq. (8) is also shown in Fig. 4(a), which closely follows the initial charge buildup. However, later in time it deviates from the prediction in equation Eq. (8), indicating that the collision rate or the relative velocities of impact between particles after charge buildup are suppressed. This is expected after mutual sticking of particles.

The conservation of charge at a single collision level and the initial condition $\sum_{i=1}^{N} q_i = 0$ results in the fact that there are statistically equal number of pairwise attractions and repulsions. This symmetry of the sign of charge among monodispersed particles has also been shown recently for a
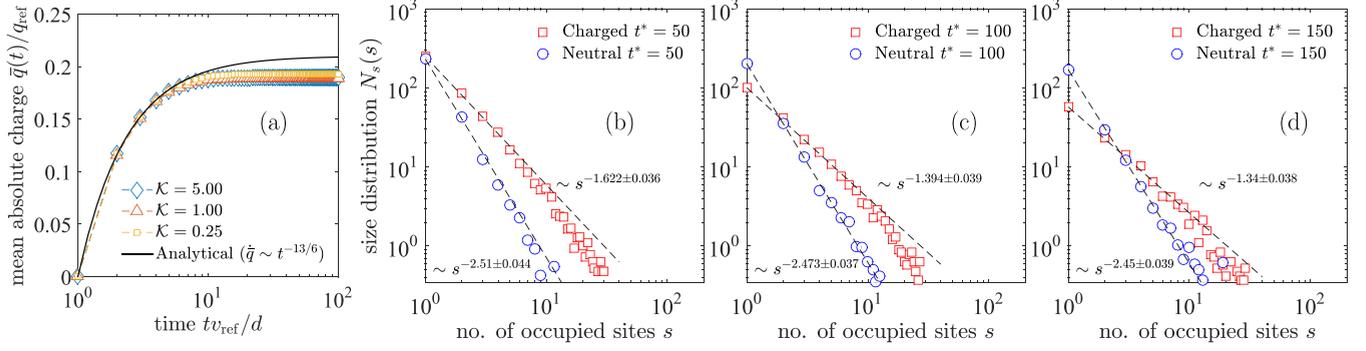
FIG. 4. (a) The evolution of mean absolute charge, $\bar{q} = \frac{1}{N} \sum_{i=1}^{N} |q_i|$, for the viscoelastic model. The mean charge saturates as a consequence of continuous reduction in the granular temperature. The solid line is the theoretical prediction in Eq. (8). (b–d) Comparison of the cluster size distribution $N_s(s)$ for charged ($\mathcal{K} = 5.0$) and neutral granular gases at different times: (b) $tv_{\text{ref}}/d = 50$; (c) $tv_{\text{ref}}/d = 100$; (d) $tv_{\text{ref}}/d = 150$, from an average over twenty independently initialized simulation runs. The dashed lines are the corresponding best fits. During the evolution of the granular gases, the slope of the distributions, or equivalently, the Fisher exponent decreases. However, the *charged* gas exhibits a more rapid decrease of the slope indicating an enhanced cluster growth (see also Fig. 5).

globally charge conserved system through experiments when no other material or wall is present [14]. As a consequence of this symmetric charge distribution, the early evolution of the granular temperature does not show any considerable deviation from the Haff's law [Fig. 1(b)]. On the other hand, if the number of pairwise repulsive interactions exceed the attractive, the rate of the decay of T_g slows down, as evident in Fig. 1(a).

A. Clustering

To investigate the statistical properties of the clusters, we calculate the cluster size distribution. A time dependent matrix which contains information about the occupied (or dense) and unoccupied (or dilute) sites in the system is obtained by thresholding the coarse-grained particle density in the system [21]. Specifically, we divide the simulation domain into equal-size boxes and, at any given time, compute the particle density in each of the boxes. The boxes which have particle density higher than a threshold value are then labeled as an "occupied site" and the rest of the boxes as "unoccupied" [61]. A cluster is then defined as the region of such connected occupied sites. This definition of clusters provides the advantage that it is independent of whether granular particles are in contact with each other in a strict sense (as they are in the charged case) or they only form density inhomogeneities without contacts (as in neutral granular gases). The size distribution $N_s(s)$ of such *connected* occupied sites is then obtained. The size distribution asymptotically scales as

$$N_s(s) \sim s^{-\tau}, \tag{9}$$

where τ is the Fisher exponent [62,63]. Figures 4(b)–4(d) shows $N_s(s)$ for both the neutral and the charged scenarios. The Fisher exponent during early aggregation increases relatively quickly in the charged case (from -1.62 to -1.34) compared to the neutral system (from -2.51 to -2.45). Additionally, the size distribution of the occupied sites is relatively broader for the charged gas. The count for a given cluster size s is larger in the charged system, except for very small s. This suggests, in relation to the observations in Fig. 2, that the clusters in the charged gas are compact and more numerous.

This difference in the rate of change of Fisher exponent in the charged system results in a different growth exponent of the so-called average cluster size,

$$S(t) = \frac{\sum_s s^2 N_s(s)}{\sum_s s N_s(s)}. \tag{10}$$

For the neutral gas, a best fit to the average over twenty independently initialized simulations reveals (Fig. 5)

$$S(t) \sim [t^{1.21 \pm 0.04} \approx t^{6/5}], \tag{11}$$
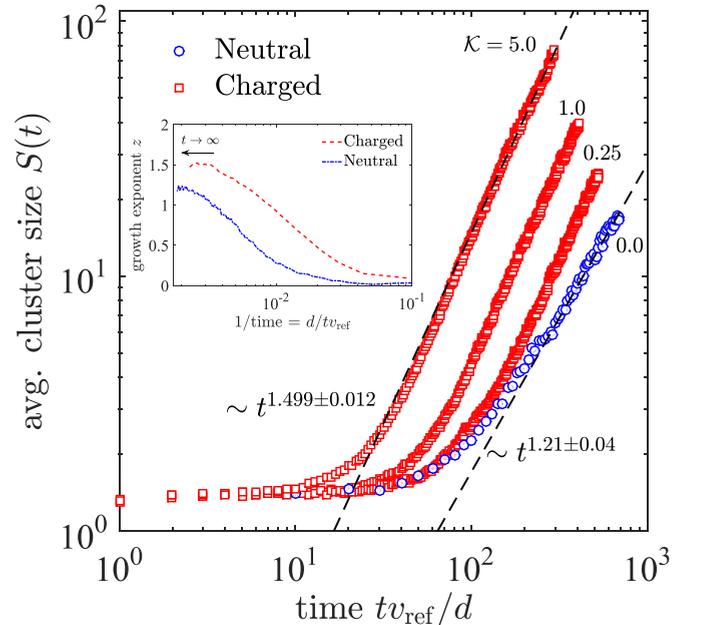
FIG. 5. Temporal dependence of the average cluster size $S(t)$, from an average over 20 independently initialized simulation runs and corresponding best fits. Granular gas with collisional charging exhibits faster growth of clusters than for neutral system. (Inset) Saturation of the growth exponent z as $1/t \to 0$ using the method of local slope. A change in the ratio of characteristic Coulomb to kinetic energy $\mathcal{K}$ does not alter the growth exponent z and only influences the crossover time of initiation of clustering.

which is close to the mean field result based on the Smoluchowski's aggregation equation [64,65]. The error in the exponent represents a 95% confidence level. For the charged gas, we obtain

$$S(t) \sim [t^{1.49 \pm 0.012} \approx t^{3/2}], \qquad (12)$$

which clearly indicates a relatively faster cluster growth (Fig. 5). The growth exponent z can be precisely obtained using the method of local slope

$$z = \frac{\log[S(t)/S(t/p)]}{\log(p)}, \qquad (13)$$

where p characterizes the time resolution [66]. In the limit $1/t \rightarrow 0$, the function should attain a saturation value, which is the best estimate for z. Figure 5 (inset) shows this saturation of z to ≈ 1.5 for the charged while to ≈ 1.21 for the neutral gas as t increases (or $1/t \rightarrow 0$).

In the charged system, the cluster growth exponent z, remarkably, does not show a dependence on the ratio of the characteristic Coulomb to kinetic energy $\mathcal{K}$ or equivalently on the typical dimensionless Bjerrum length ℓ_B/d. In Fig. 5 we show $S(t)$ for increasing $\mathcal{K} = 0.25$, 1.0 and $\mathcal{K} = 5.0$. Upon decreasing $\mathcal{K}$, the characteristic time t_c for the emergence of aggregation increases and approaches the neutral case as $\mathcal{K} \rightarrow 0$. However, once the aggregation starts, it does not influence the growth exponent z. An increase of t_c upon decreasing $\mathcal{K}$ is reminiscent of the self-focusing Brownian aggregation of *monopolarly* charged particles found in Ref. [20].

B. Mean field

Aggregation phenomena are very common in nature, for example, coalescence of rain drops, coagulation of snow, aerosol and powders, polymerization, or agglomeration in colloids. One is often interested in determining, at a given time during the aggregation process, the sizes of the aggregates and the rate at which they grow in time. A simple way to approach is via mean-field theory, which has been extensively applied (mainly for uncharged particle systems) to precisely predict the time dependent aggregate size distributions and their growth rate by taking into account only the crudest features of the underlying transport processes and the nature of the physical interactions between the aggregates. Smoluchowski's coagulation equation is one such approximation. Here we make a mean-field approximation of the aggregation of the initially monodisperse system using the Smoluchowski's equation

$$\frac{\partial n(i,t)}{\partial t} = \frac{1}{2} \sum_{j=1}^{i-1} K_a(j, i-j) n(j,t) n(i-j,t)$$

$$- n(i,t) \sum_{j=1}^{\infty} K_a(j,i) n(j,t), \qquad (14)$$

where $n(i,t)$ is the number density of aggregate of size i in the system at time t, and $K_a(j,i)$ is the aggregation kernel. The kernel $K_a(j,i)$ is typically related to the collision cross-section $\sigma(j,i)$ of the colliding aggregates and the relative aggregate velocity $v(j,i)$ as [67]

$$K_a(j,i) \propto \sigma(j,i) v(j,i). \qquad (15)$$

The collision-cross section is typically dependent on the aggregate size while the velocity part of the kernel is related to the diffusion of the aggregates. Numerical solution of Eq. (14) with a well-known kernel of the form

$$K_a(j,i) \propto (i^{1/3} + j^{1/3})^2 (i^{-1} + j^{-1})^{1/2} \qquad (16)$$

from the kinetic theory of *uncharged* particle aggregation [68] yields a growth exponent $z = 1.19$, which is close to our result for the neutral case in Fig. 5.

Electrostatic interactions are difficult to treat as they result in an additional dependence of K_a on the charge distribution among the aggregates besides the dependence on the size distribution. It is, however, possible to include the effects of electrostatic interactions in the aggregation kernel [20,69]. If the charge on the individual particles is time dependent and fluctuating, as in the present study, even the solution of the above mean-field theory becomes quite complex. As a first attempt for a collisionally charged granular gas, here we indirectly introduce the electrostatic effects in the Smoluchowski's kernel K_a based on the results from the MD simulations. Under this, for a *bipolarly* charged gas, we argue that the average collision cross-section $\langle \sigma(j,i) \rangle$ remains statistically unchanged due to the symmetry of the charge distribution. This is true as long as the net charge in the system is zero. This conjecture is consistent with the result in Fig. 1(b), which shows no significant deviation of T_g from the neutral system, at least in the early stage of evolution. However, the relative aggregate velocities $v(j,i)$ are expected to be suppressed due to the mutual sticking of particles and their entrapment in the electrostatic field, as discussed previously. This fact is modeled in the kernel by introducing a variable β as

$$K_a(j,i) \propto (i^{1/3} + j^{1/3})^2 (i^{-1} + j^{-1})^{1/\beta}, \qquad (17)$$

where $\beta = 2$ corresponds to the neutral aggregation. An increasing β simply implies a suppressed diffusion. We numerically solve the Smoluchowski's equation with the kernel Eq. (17). The growth exponent $z \rightarrow 1.49$ when $\beta \rightarrow 3$. The increase in the value of z in the mean-field theory when the velocity term $v(j,i)$ is suppressed supports the argument of reduction in the relative aggregate velocities.

To support the inclusion of the parameter β in the diffusion part of the kernel, we study the mean square displacement (MSD) of the particles. This is depicted in Fig. 6. The MSD in a dissipative granular gas is known to exhibit a subdiffusive behavior [56]. Figure 6 (inset) shows that the subdiffusive regime due to dissipation is further suppressed due to the electrostatic interactions. The fact that the MSD is strongly subdiffusive is consistent with a reduced relative aggregate velocities and thus with increasing β.

The Smoluchowski's equation can be further simplified, if a strict monodisperse mass distribution of the aggregates is assumed at any time t, i.e., at a given time t, only aggregates with size i are present and the number density of aggregates of size j other than i is zero. This approximation is rather severe; however, it reduces the Smoluchowski's equation to an analytically solvable form, written as [67]

$$\frac{\partial n(i,t)}{\partial t} = -K_a(i,i) n^2(i,t), \qquad (18)$$
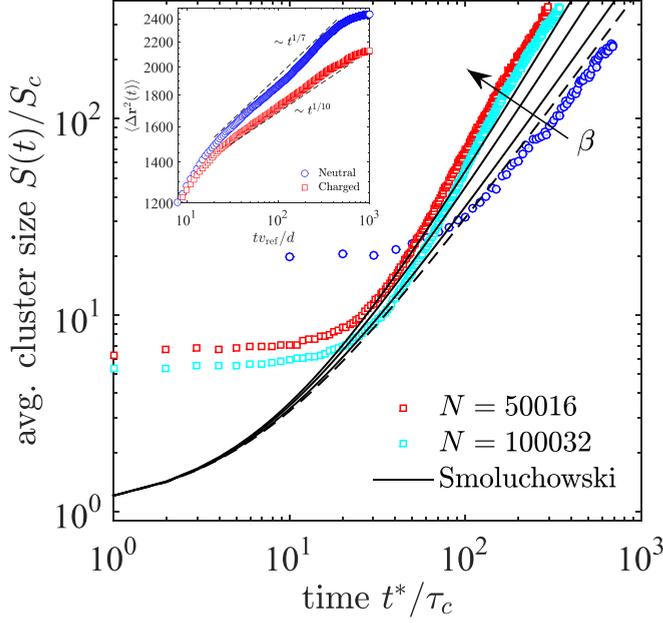
FIG. 6. Comparison of the average cluster size $S(t)$ predicted by the Smoluchowski equation with the MD results. At $\beta = 2$ (dashed line) the mean-field solution agrees reasonably well with the neutral gas, while as $\beta \to 3$ (solid lines) the growth rate for the charged granular gas is recovered. (Inset) Comparison of the MSD of particles between the charged and the neutral gas. The sub-diffusion due to dissipation is further suppressed by the electrostatics, which in the mean-field approximation is modeled by increasing β. Here S_c and τ_c are factors used to shift the curves and plot them close to each other for the sake of comparison of the slopes.

where the kernel $K_a(i,i)$ now takes the following form:

$$K_a(i,i) \propto (i^{1/3})^2 (i^{-1})^{1/\beta} = i^{1/6} i^{-1/\beta}. \quad (19)$$

If the total mass in the system is conserved, then $n(i,t)i(t) = $ const., and one can transform Eq. (18) to the following:

$$\frac{\partial i(t)}{\partial t} = \frac{1}{\tau_o}(i^{1/6} i^{-1/\beta}), \quad (20)$$

where τ_o is some characteristic time. The solution of this ordinary, but nonlinear differential equation is

$$i(t) \sim t^z, \text{ with } \begin{cases} z = 6/5, & \text{if } \beta = 2, \\ z > 6/5, & \text{if } \beta > 2, \\ z = 3/2, & \text{if } \beta = 3. \end{cases} \quad (21)$$

Figure 6 also shows the comparison of Eq. (21) with the MD results. Upon changing β from 2 to 3 the mean-field calculations agree reasonably well with the MD results, which is consistent with the suppression of diffusivity due to electrostatics [Fig. 6 (inset)]. We find that the system size does not affect our results. Here it should be noted that the size/mass $i(t)$ scales linearly with the average size of the occupied sites $S(t)$ by definition. The consistency of the results from numerically solving the kernel in Eq. (17), MD calculations, and Eq. (21) suggest that the suppression of particle diffusion due to electrostatics enhances the aggregation process.
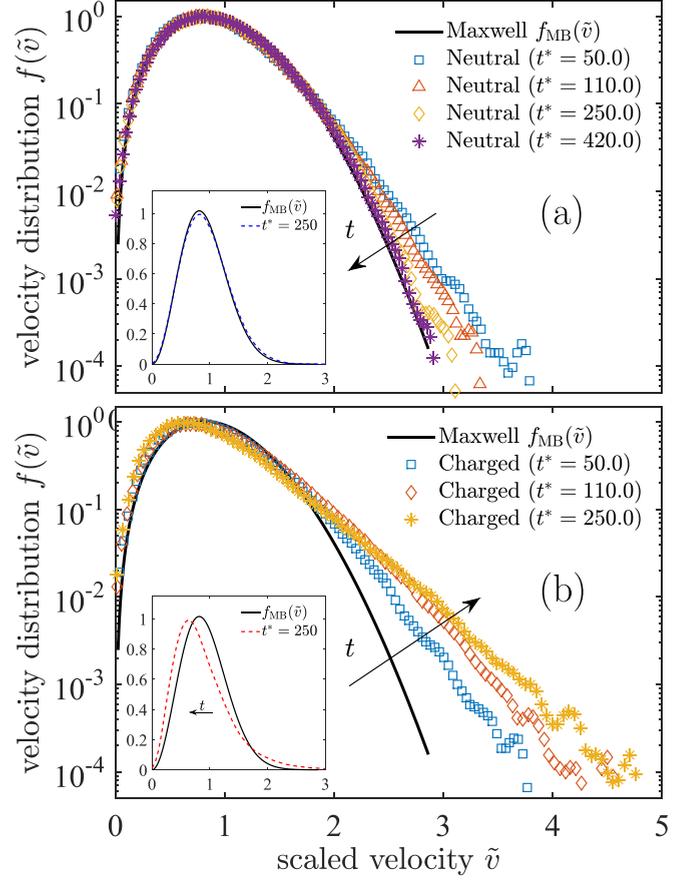
FIG. 7. (a) The relaxation of the scaled velocity ($\tilde{v} = v/\langle v^2 \rangle^{1/2}$) distribution function toward the Maxwellian for neutral viscoelastic particles. This result from our simulations for neutral viscoelastic particles is consistent with the Sonine expansion for the time dependent distribution function [50], which depicts that the distribution relaxes back toward the Maxwellian in the long time limit. (b) The time evolution of the distribution $f(\tilde{v})$ for a charged system, however, shows a behavior opposite to the neutral case: the distribution does not relax back to the Maxwellian. (Insets) Same results as in (a) and (b) but on a linear scale to highlight the shift of the most probable velocity for the charged granular gas.

C. Velocity distribution

To analyze the global effects of charging on the dynamical state of the system, we also study the evolution of the normalized velocity distribution function $f(\tilde{v})$, where $\tilde{v} = v/\langle v^2 \rangle^{1/2}$, and its deviation from the equilibrium, Maxwellian distribution $f_{MB}(\tilde{v})$. For viscoelastic particles $f(\tilde{v})$ quickly deviates from the Maxwell distribution early in time, attains a maximal deviation regime and tends to approach back the Maxwellian [50]. This behavior for neutral viscoelastic particles is shown in Fig. 7(a), where the relaxation of $f(\tilde{v})$ after its maximal deviation is highlighted. The physical reasoning behind this relaxation is that as $t \to \infty$, the impact velocities $\dot{\xi}_{ij}$ tend to reduce which implies the coefficient of restitution $\epsilon = (\dot{\xi}'_{ij}/\dot{\xi}_{ij}) \to 1$. This causes most collisions to be effectively elastic and thus $f(\tilde{v},t) \to f_{MB}(\tilde{v})$ [70]. The intriguing finding in our study is that the deviation of $f(\tilde{v})$ from the Maxwellian is more significant in dynamically charged systems and it
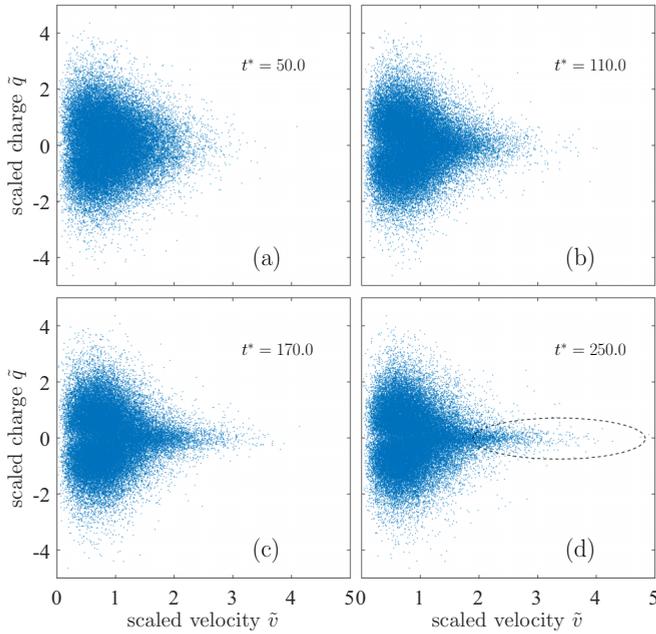
FIG. 8. Scatter plot of the particles' charges and velocities at different times. As time progresses, a subpopulation of high velocity, nearly neutral particles develops (highlighted in the dashed ellipse), which contributes to the exponential tails in the velocity distribution function (see Fig. 7). This subpopulation is expected to cause the occasional fragmentation of the local aggregates (see Fig. 3). Here, $\tilde{q} = q/\langle q^2 \rangle^{1/2}$ and $\tilde{v} = v/\langle v^2 \rangle^{1/2}$.

does not exhibit a relaxation toward $f_{\mathrm{MB}}(\tilde{v})$ within the early stage of aggregation. Figure 7(b) shows $f(\tilde{v})$ at different times for a charged system. The deviation of $f_{\mathrm{MB}}(\tilde{v})$ from $f(\tilde{v})$ is more pronounced in the charged case than in the neutral gas and indicates that the nature of the clustering is different in case of dynamically charged systems as compared to the neutral system. The tail of the distribution nearly scales as $f(\tilde{v}) \sim \exp(-\tilde{v})$ in both cases. Over time, the most probable value of $\tilde{v}$ is reduced in the charged system [Fig. 7(b) (inset)]. On the other hand, this deviation is minimal for the neutral gas particles [Fig. 7(a) (inset)]. The difference between the two cases again indicates a reduced motility of particles in the charged gas.

The high speed particles from the tail of $f(\tilde{v})$ compensate the reduction of the most probable velocity. To understand which particles are—statistically—responsible for the fat exponential tail of the distribution, we consider a scatter plot of charge and speed for our system, as shown in Fig. 8. As the time elapses, a subpopulation of weakly charged particles with high velocities can be identified. This subpopulation corresponding to the fat tail of the distribution suggests an interesting and counterintuitive fact. Although the tail of the distribution deviates significantly from $f_{\mathrm{MB}}(\tilde{v})$ in the charged systems, weakly charged particles are actually responsible for it. These weakly charged and high speed particles fail to stick and form agglomerates. It can be imagined that these particles experience fewer collisions due to the fact that more space is provided by the agglomeration process. Thus, the nonequilibrium nature of the charged granular gas is enhanced indirectly through the agglomerating particles and

directly by the weakly charged, high-speed particles. This scenario implies a thermal decoupling between highly charged particles and the subpopulation of weakly charged particles. We expect that due to their relatively high velocities, these weakly charged particles are then the most probable reason behind the occasional fragmentation of the local aggregates, as observed in Fig. 3. In neutral freely cooling granular gases, the exponential tails of the velocity distribution during the intermediate time regime are dominated by the fastest moving particles which manage to avoid any collision with other particles [49]. However, the number of such particles decreases over time and eventually the large-velocity tail tends to diminish [49]. In the present scenario, the "survival probability" of such uncharged fastest-moving particles is expected to be higher as they gain more accessible volume due to the compact coagulation of the other charged particles. Consequently, the large-velocity tail survives, at least during the early-stages of the particle aggregation.

IV. CONCLUSIONS

We have studied the effect of *collisional* charging on the aggregation dynamics of dilute, freely cooling granular gases of viscoelastic particles. We perform molecular dynamics simulations that take into account the collisional charge exchange, and the electrostatic interactions by means of the Ewald summation. Our simulations depict that the electrostatic interactions due to collisional charging alter the morphology and the growth rate of the clusters. In a charged system, the local sticking of particles triggers the aggregation, and the subsequent growth of the average cluster size is enhanced. The growth of the average cluster size is found to be independent of the ratio of characteristic Coulomb to kinetic energy, or equivalently, of the typical Bjerrum length. The combined results from the numerical solution of Eq. (14) with the kernel in Eq. (17), the results in Eq. (21), the behavior of $f(\tilde{v})$ as shown in Fig. 7(b), and the MD results all suggest that electrostatic interactions enhance the aggregation process in a charged granular gas.

In our work, some important physical ingredients such as friction, rotational degrees of freedom of the particles as well as other charging mechanisms such as ionization of the particle interstitial gas due to irradiation, are not included. Especially important is to further improve the charge exchange model [Eq. (3)]. However, our study, we believe, will be helpful in clarifying very basic feature of natural processes which produce dust aggregation in charged environments *e.g.*, the agglomeration of planetary dust [25] and cohesive powder substructures [27]. In the perspective of planetary dust aggregation, it will also be interesting to include the effects due to drag caused by interstitial gas surrounding the particles, dipolar effects [4,71], as well as van der Waals effects [25].

[1] R. Anderson, S. Björnsson, D. C. Blanchard, S. Gathman, J. Hughes, S. Jónasson, C. B. Moore, H. J. Survilas, and B. Vonnegut, Science **148**, 1179 (1965).

[2] G. W. Most, *Hesiod: Theogony, Works and Days, Testimonia* (Harvard University Press, Cambridge, MA, 2006), Vol. 1.

[3] E. W. B. Gill, Nature **162**, 568 (1948).

[4] P. S. Wesson, Astrophys. Space Sci. **23**, 227 (1973).

[5] T. Poppe, J. Blum, and T. Henning, Astrophys. J. **533**, 472 (2000).

[6] W. D. Crozier, J. Geophys. Res. **69**, 5427 (1964).

[7] G. Simpson and F. J. Scrase, Proc. R. Soc. London A **161**, 309 (1937).

[8] A. K. Kamra, Nature **240**, 143 (1972).

[9] R. Franz, R. Nemzek, and J. Winckler, Science **249**, 48 (1990).

[10] J. Blum and G. Wurm, Annu. Rev. Astron. Astrophys. **46**, 21 (2008).

[11] J. Kolehmainen, A. Ozel, C. M. Boyce, and S. Sundaresan, AIChE J. **62**, 2282 (2016).

[12] M. Nifuku, T. Ishikawa, and T. Sasaki, J. Electrost. **23**, 45 (1989).

[13] A. G. Bailey, J. Electrost. **45**, 85 (1998).

[14] V. Lee, S. R. Waitukaitis, M. Z. Miskin, and H. M. Jaeger, Nat. Phys. **11**, 733 (2015).

[15] W. Hu, L. Xie, and X. Zheng, Appl. Phys. Lett. **101**, 114107 (2012).

[16] F. Nordsiek and D. P. Lathrop, arXiv:1509.04214 (2015).

[17] R. Yoshimatsu, N. A. M. Araújo, G. Wurm, H. J. Herrmann, and T. Shinbrot, Sci. Rep. **7**, 39996 (2017).

[18] T. Scheffler and D. E. Wolf, Granular Matter **4**, 103 (2002).

[19] M.-K. Müller, *Long-range Interactions in Dilute Granular Systems* (University of Twente, Enschede, The Netherlands, 2008).

[20] S. M. Dammer and D. E. Wolf, Phys. Rev. Lett. **93**, 150602 (2004).

[21] S. Paul and S. K. Das, Phys. Rev. E **96**, 012105 (2017).

[22] P. Das, S. Puri, and M. Schwartz, Phys. Rev. E **94**, 032907 (2016).

[23] K. C. Pingali, S. V. Hammond, F. J. Muzzio, and T. Shinbrot, Int. J. Pharm. **369**, 2 (2009).

[24] A. Mehrotra, F. J. Muzzio, and T. Shinbrot, Phys. Rev. Lett. **99**, 058001 (2007).

[25] J. Blum, G. Wurm, S. Kempf, T. Poppe, H. Klahr, T. Kozasa, M. Rott, T. Henning, J. Dorschner, R. Schräpler *et al.*, Phys. Rev. Lett. **85**, 2426 (2000).

[26] T. Poppe, J. Blum, and T. Henning, Astrophys. J. **533**, 454 (2000).

[27] T. Schwager, D. E. Wolf, and T. Pöschel, Phys. Rev. Lett. **100**, 218002 (2008).

[28] S. Miller and S. Luding, Phys. Rev. E **69**, 031305 (2004).

[29] S. Luding and H. J. Herrmann, Chaos **9**, 673 (1999).

[30] N. Brilliantov, P. L. Krapivsky, A. Bodrova, F. Spahn, H. Hayakawa, V. Stadnichuk, and J. Schmidt, Proc. Natl. Acad. Sci. U.S.A. **112**, 9536 (2015).

[31] N. V. Brilliantov and F. Spahn, Math. Comput. Simulat. **72**, 93 (2006).

[32] E. Murphy and S. Subramaniam, Phys. Fluids **27**, 043301 (2015).

[33] S. Takada, K. Saitoh, and H. Hayakawa, Phys. Rev. E **94**, 012906 (2016).

[34] G. Kuwabara and K. Kono, Jpn. J. Appl. Phys. **26**, 1230 (1987).

[35] N. V. Brilliantov, F. Spahn, J.-M. Hertzsch, and T. Pöschel, Phys. Rev. E **53**, 5382 (1996).

[36] T. Pöschel and T. Schwager, *Computational Granular Dynamics: Models and Algorithms* (Springer Science & Business Media, Berlin, 2005).

[37] Taking silica particles as representative for the granular gas fixes Young's modulus $Y = 73.1$ GPa, Poisson's ratio $\nu = 0.2$, particle mass density $\rho = 2650$ kg/m^3. We select a small value of the dissipation constant $A = 7.0 \times 10^{-6}$ s. The thermal energy scale or the initial granular temperature is $T_0 = 10$. If we consider particle size $d = \mathcal{O}(\text{mm})$, we find $\mathcal{E} \approx 278.6$, $\mathcal{D} \approx 27.7$. In all our calculations we fix $\mathcal{E} = 278.6$, $\mathcal{D} = 27.7$.

[38] A. P. Johnson, H. J. Cleaves, J. P. Dworkin, D. P. Glavin, A. Lazcano, and J. L. Bada, Science **322**, 404 (2008).

[39] G. D. Freier, J. Geophys. Res. **65**, 3504 (1960).

[40] C. D. Stow, Weather **24**, 134 (1969).

[41] D. J. Lacks and R. M. Sankaran, J. Phys. D: Appl. Phys. **44**, 453001 (2011).

[42] O. Melnik and M. Parrot, J. Geophys. Res. **103**, 29107 (1998).

[43] M. Glor, J. Electrost. **16**, 175 (1985).

[44] Y. Pu, M. Mazumder, and C. Cooney, J. Pharm. Sci. **98**, 2412 (2009).

[45] T. Pähtz, H. J. Herrmann, and T. Shinbrot, Nat. Phys. **6**, 364 (2010).

[46] S. Takada, D. Serero, and T. Pöschel, Phys. Fluids **29**, 083303 (2017).

[47] T. Poppe and R. Schräpler, Astron. Astrophys. **438**, 1 (2005).

[48] D. Frenkel and B. Smit, *Understanding Molecular Simulation: From Algorithms to Applications* (Academic Press, San Diego, CA, 2001), Vol. 1.

[49] X. Nie, E. Ben-Naim, and S. Chen, Phys. Rev. Lett. **89**, 204301 (2002).

[50] N. V. Brilliantov and T. Pöschel, *Kinetic Theory of Granular Gases* (Oxford University Press, Oxford, 2010).

[51] E. L. Grossman, T. Zhou, and E. Ben-Naim, Phys. Rev. E **55**, 4200 (1997).

[52] K. van der Weele, D. van der Meer, M. Versluis, and D. Lohse, Europhys. Lett. **53**, 328 (2001).

[53] R. Mikkelsen, D. van der Meer, K. van der Weele, and D. Lohse, Phys. Rev. Lett. **89**, 214301 (2002).

[54] E. Ben-Naim and P. L. Krapivsky, Phys. Rev. E **61**, R5 (2000).

[55] D. ben-Avraham, E. Ben-Naim, K. Lindenberg, and A. Rosas, Phys. Rev. E **68**, 050103(R) (2003).

[56] A. S. Bodrova, A. V. Chechkin, A. G. Cherstvy, H. Safdari, I. M. Sokolov, and R. Metzler, Sci. Rep. **6**, 30520 (2016).

[57] N. V. Brilliantov and T. Pöschel, Phys. Rev. E **61**, 1716 (2000).

[58] A. Bodrova, A. V. Chechkin, A. G. Cherstvy, and R. Metzler, Phys. Chem. Chem. Phys. **17**, 21791 (2015).

[59] K. Harth, T. Trittel, S. Wegner, and R. Stannarius, arXiv:1706.07472.

[60] P. K. Haff, J. Fluid Mech. **134**, 401 (1983).

[61] The threshold filling fraction is taken equal to a third of the maximum possible filling fraction, that is, the hexagonal close packing for equal spheres, $\phi_{\text{hcp}} = \frac{\pi}{3\sqrt{2}} = 0.7405$. Changing the threshold in our calculations only results in a different multiplicative factor for the average cluster size, and does not change the growth exponents.

[62] D. Stauffer, Phys. Rep. **54**, 1 (1979).

[63] D. Stauffer and A. Aharony, *Introduction to Percolation Theory* (Taylor & Francis, London, 2003).

[64] F. Leyvraz, Phys. Rep. **383**, 95 (2003).

[65] S. N. Pathak, Z. Jabeen, D. Das, and R. Rajesh, Phys. Rev. Lett. **112**, 038001 (2014).

[66] S. Lübeck, Int. J. Mod. Phys. B **18**, 3977 (2004).

[67] J. Blum, Adv. Phys. **55**, 881 (2006).

[68] S. J. Antony, W. Hoyle, and Y. Ding, *Granular Materials: Fundamentals and Applications* (Royal Society of Chemistry, London, 2004).

[69] A. V. Ivlev, G. E. Morfill, and U. Konopka, Phys. Rev. Lett. **89**, 195502 (2002).

[70] T. Pöschel, N. V. Brilliantov, and T. Schwager, Physica A **325**, 274 (2003).

[71] T. Siu, W. Pittman, J. Cotton, and T. Shinbrot, Granular Matter **17**, 165 (2015).